

**AUSTENITIZATION OF LAMELLAR PEARLITE IN 100CrMnSi6-4 BEARING STEEL**DLOUHY Jaromír<sup>1</sup>, MOTYCKA Petr<sup>1</sup><sup>1</sup>COMTES FHT a.s., Dobřany, Czech Republic, EU, [Jaromir.dlouhy@comtesfht.cz](mailto:Jaromir.dlouhy@comtesfht.cz)**Abstract**

It is well known, that lamellar pearlite austenitization can lead to rapid spheroidisation of cementite. This phenomenon is the base for ASR process - Accelerated carbide Spheroidisation and Refinement. It is possible to obtain fully spheroidised structure from lamellar pearlite within minutes by partial austenitization and divorced pearlitic transformation. Moreover, such structure is significantly finer than spheroidised structure after conventional soft annealing. The size of carbide particles obtained by ASR process depends on the austenitization rate. This is an important fact, because various kinds of heating methods can be applied for steel heat treatment with heating rate differing by decade orders. This article describes cementite morphology during spheroidisation with respect to the austenitization kinetics.

100CrMnSi6-4 with pearlitic structure was austenitized isothermally at different temperatures and continuously at different heating rate. Cementite lamellae fragmentation at interphase boundary perlite/austenite was examined by SEM after deep etching. Size and distribution of resulting cementite fragments was characterized. Austenitization kinetics was observed via dilatometric measurement.

**Keywords:** Carbide spheroidisation, bearing steel, pearlite, austenitization

**1. INTRODUCTION**

Austenitization of pearlite is basic structural transformation occurring in wide variety of thermal treatment, from soft annealing to the quenching [1]. Mechanism and kinetic of austenitization is not so important in cases of full austenitization resulting in homogeneous austenite in equilibrium state. Its mechanism however plays crucial role in case of incomplete austenitization or nonequilibrium states, because it determines final structure of such incomplete and/or rapid austenitization. Nonequilibrium austenitization occurs e.g. during induction hardening with high heating rates, followed by quenching. Equilibrium, but partial austenitization occurs during austenitization of hypereutectoid steels, where undissolved carbides are left in austenitic matrix intentionally as obstacles for the austenite grain growth or as wear-resistant particles in final hardened structure.

Rapid, i.e. unequilibrium, austenitization can result in rapid spheroidisation of pearlitic cementite lamellae [2]. This phenomenon called Accelerated carbide Spheroidisation and Refinement (ASR) was extensively studied at bearing steel of grade 100CrMnSi6-4. Major concern was to replace conventional spheroidisation (soft) annealing by ASR process. Finer cementite globules after ASR process caused finer structure after subsequent hardening in comparison with soft annealed structure, as well as higher hardness. The ASR phenomenon is based on rapid partial austenitization (full austenitization of pearlitic ferrite, but only partial cementite dissolution) and subsequent divorced pearlitic transformation [3].

Cementite lamellae partial dissolution results in their fragmentation. Mechanism of lamellae fragmentation was described in study of Shtansky et al. [4]. Presented article describes dependence of lamellae fragmentation period - fragments spacing - on austenitization rate. This is important for controlling of size and spatial density of resulting cementite globules after ASR process.

**2. MATERIAL AND METHODS**

The experimental material was 100CrMnSi6-4 bearing steel with chemical composition given in **Table 1**. The steel was delivered in hot rolled condition in form of bars 21 mm in diameter. Bars were cooled in air after

rolling. Steel microstructure was pearlitic with small amount of secondary cementite on the prior austenite grain boundaries.

**Table 1** Chemical composition of the experimental steel

Element	C	Mn	Si	Cr	Ni	Cu	P	S	Fe
wt. %	1.02	1.26	0.57	1.55	0.03	0.02	0.02	0.02	bal.

Thermal treatment was performed in quenching dilatometer Linseis L78 RITA. It enables dilatometric analysis of metallic cylindrical samples from 3 to 5 mm in diameter and typically 10 mm in length. Samples are heated by induction heating and cooled by gas flow. Maximal controlled cooling and heating rate is 200 °C / s. Dilatometers chamber was evacuated and filled with argon. Specimens for heat treatment in the dilatometer were prepared in form of cylinders 4mm in diameter and 10 mm in length. **Figure 1** shows initial pearlitic structure.

Two series of regimes (**Table 2**) were carried out - regimes with austenitization during isothermal hold and during continuous heating. The dilatometric records were analysed, and the second round of experiment was performed. All regimes were repeated for both sample series and austenitization was interrupted by rapid cooling with cooling velocity higher than 200 °C / s in a moment, when austenite formed only ca 10 vol. % of the sample volume. Austenite transformed into martensite and cementite morphology remained "frozen" in state during austenitization. Thus it was possible to study cementite morphology on the pearlite/austenite interphase.

**Table 2** List of examined regimes with sample labelling (**in bold**)

Regimes labelling	Isothermal austenitization - - heating 140 °C / s, isothermal hold		Continuous heating - - rates 2, 10, 50 and 140 °C / s.	
	Isothermal hold to the equilibrium (°C)	Isothermal hold to the estimated 10 vol. % of austenite, quenching (°C)	Heating to the 900°C (°C / s)	Heating to the estimated 10 vol. % of austenite, quenching (°C / s)
750	<b>Q750</b> (260sec)		<b>2</b>	<b>Q2</b> (775°C)
760	<b>Q760</b> (22.5sec)		<b>10</b>	<b>Q10</b> (792°C)
770	<b>Q770</b> (9.5sec)		<b>50</b>	<b>Q50</b> (813°C)
780	<b>Q780</b> (3.4sec)		<b>140</b>	<b>Q140</b> (834°C)
790				
800				
810				

Longitudinal metallographic sections were prepared in axis of all quenched samples by mechanical grinding and polishing. Microstructure was revealed by etching in Nital solution. Deep etching was performed to reveal



**Figure 1** Optical micrograph - initial pearlitic structure of the experimental steel

3D morphology of fragmenting cementite lamellae. Microstructure was observed in scanning electron microscope JEOL JSM 7400F. Areas with pearlitic lamellae fragmentation into parallel rods were found and distance between the rods was measured. Measurement was performed in image analysis software Nis Elements.

### 3. RESULTS AND DISCUSSION

Metallographic observation of growing austenite was performed on quenched samples with interrupted austenitization. Austenite nucleated almost exclusively on pearlite colonies boundaries, as seen in **Figure 2**. It shows growing austenite grain, clearly visible in standardly etched metallographic section. Fast cooling turned austenite into martensite. Martensite etching rate is several times slower than it is for ferrite, thus martensite remains almost unetched while ferrite is removed by etching into significant depth. Thus former austenite, now martensite, areas appears to rise above level of etched ferrite. Cementite remains unaffected by Nital solution and its lamellae and particles reaches on the level of original unetched section surface.

**Figure 3** depicts detail of growing austenite grain into lamellar perlite. Austenite grows into ferritic lamellas and is constrained by cementitic lamellas from sidewise growth (see arrow in **Figure 3**). There are clearly visible cementite particle in newly formed austenite grain. They formed from original pearlitic lamellae of cementite. Lamellae fragmentation was studied after deep etching of the sample.

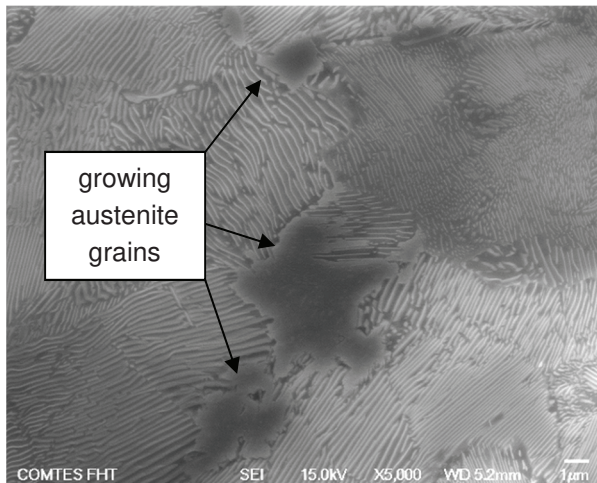


**Figure 2** Sample Q760 °C - growing austenite on pearlitic colonies boundary

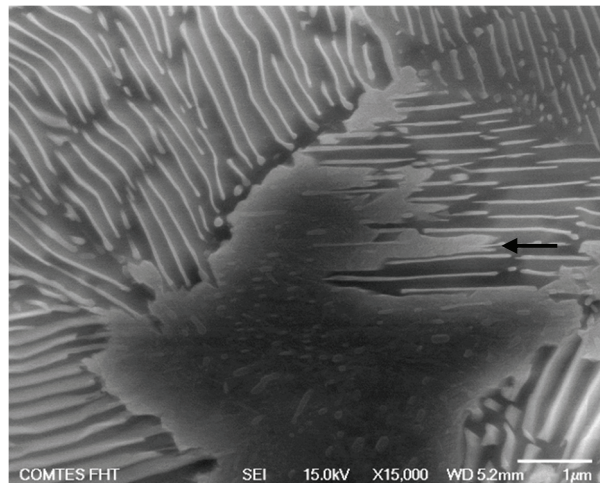


**Figure 3** Detail of growing austenite

3D morphology of cementite lamellae is shown in **Figures 4** and **5**. At some places, fragmentation resulted in array of parallel cementite cylinders with almost perfect circular cross section (**Figure 4**). **Figure 4** shows clearly also martensitic matrix, formed from austenite during cooling. Lamellae at fragmentation beginning can be seen on the left side of the figure. The fragmentation took place at very narrow zone at austenite front ca 1 µm wide. **Figure 4** shows area, where cementite fragmentation lead to the array of parallel rods. Such areas was chosen for "fragmentation period" measurement - measurement of an average distance between adjacent cementite rods.

Initially planar lamellae changed mostly into irregular interconnected lace-like nets (**Figure 5**). This figure shows pearlite colony boundary (dotted line). Colony on the right upper corner is intact and austenite grew only to the colony filling rest of the picture.



**Figure 4** Sample Q2 °C / s - lamellae fragmentation into parallel rods

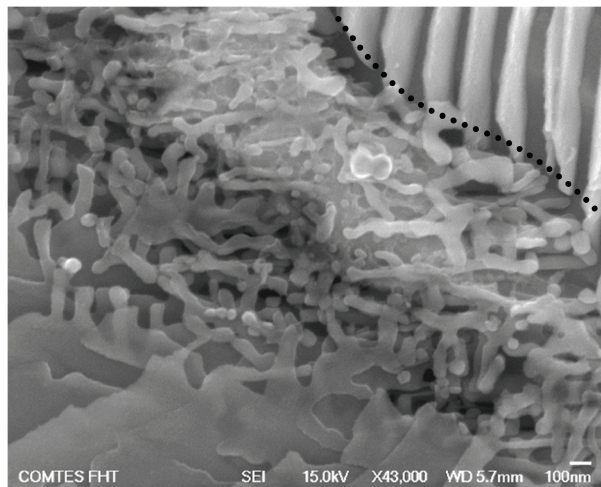


**Figure 5** Sample Q140 °C / s - lamellae fragmentation into irregular shapes

Fragmentation period measurements showed the same trend for both isothermal and anisothermal austenitization (**Figure 6**). Fragments spacing decreases with increasing transition temperature. Dilatometric analysis (**Figure 7**) showed kinetics of the  $\alpha \rightarrow \gamma$  transition, which shows indirectly the velocity of austenite/ferrite interphase movement. Fragmentation period is probably not bound only to the temperature, but significantly to the rate of interphase movement.

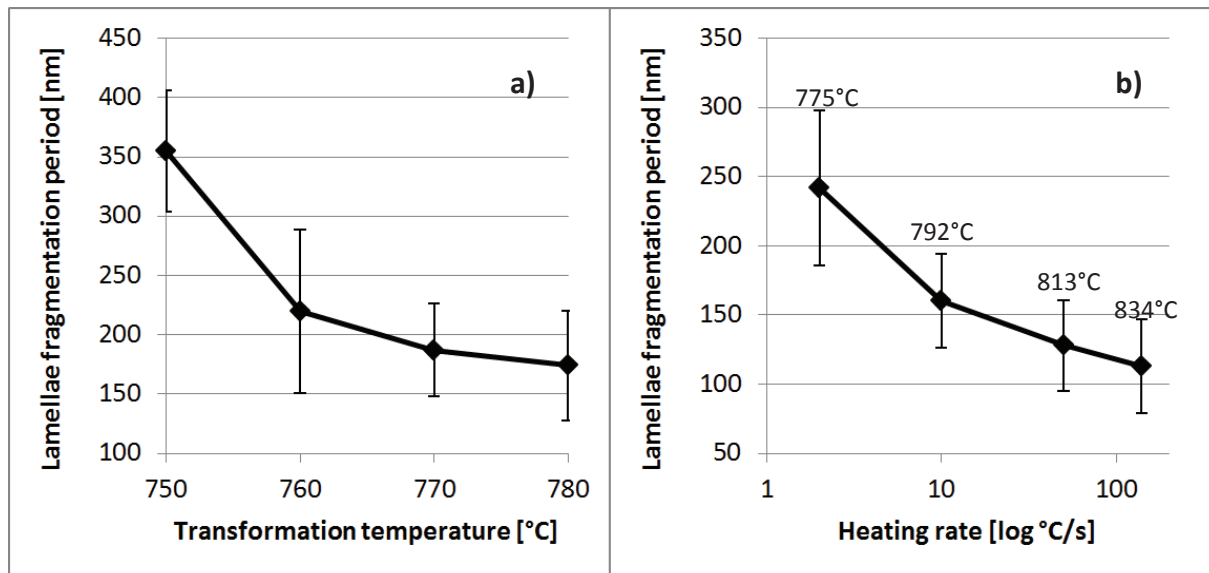


**Figure 6** Effect of a) temperature of isothermal austenitization, b) heating rate, on average distance of cylindrical lamellae fragments. Temperatures, where heating was interrupted at anticipated 10 vol. % of austenite, are stated in b)

Dilatometric record for isothermal austenitization is shown in **Figure 7**. Typical shape of the curve of phase transformation can be seen for austenitization at 810°C. Austenitization regime was stopped for sample 750 °C after one hour, because only ca 40% of pearlite had austenitized. Austenitization at temperatures 760 °C - 800 °C was retarded before full  $\alpha \rightarrow \gamma$  transformation. Arrows in **Figure 7** show moments of transformation retardation, when the kinetics of the transformation changed its character. This behaviour reflects the change in controlling mechanism of  $\alpha \rightarrow \gamma$  transformation.

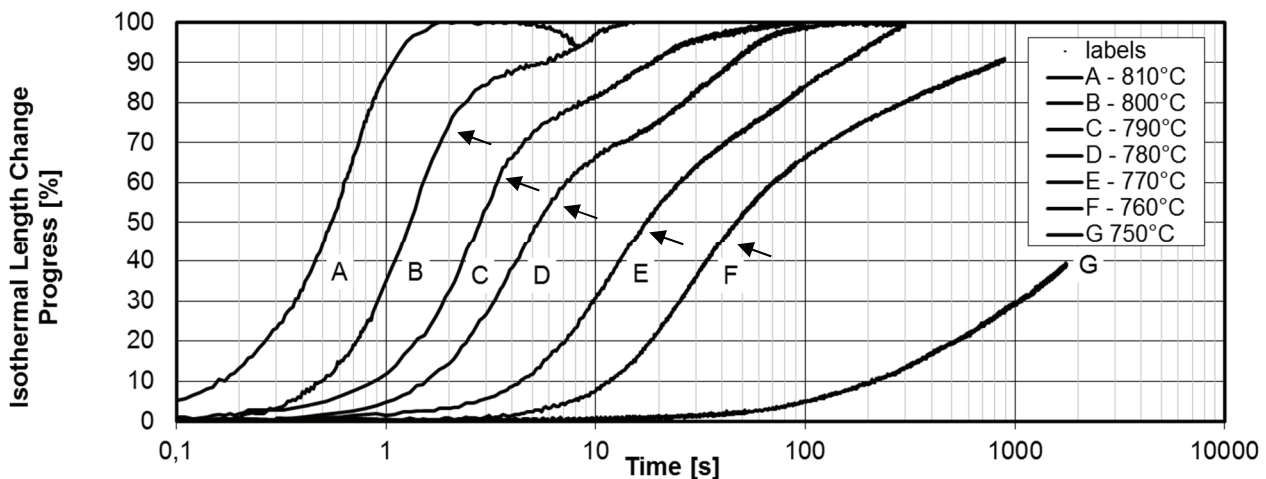


**Figure 7** Dilatometric curves of austenitization during isothermal hold for various temperatures. 100% on the y-axis represents maximal contraction of the sample caused by  $\alpha \rightarrow \gamma$  transformation

Initially, the  $\alpha \rightarrow \gamma$  transformation is controlled by carbon diffusion. Cementite lamellae dissolves, carbon diffuses to the austenite/ferrite interface and enables its movement. Cementite dissolution is retarded by chromium, which is concentrated in cementite. Chromium stabilizes the cementite and after certain degree of cementite dissolution via carbon diffusion, chromium diffusion is also required [5, 6]. Diffusion of chromium is much slower than carbon diffusion, thus whole process of cementite dissolution and  $\alpha \rightarrow \gamma$  transformation is retarded. Curve A in **Figure 7** shows no retardation of the phase transition, thus it can be assumed, that its kinetic is controlled only by carbon diffusion. Sample expansion was observed after finished  $\alpha \rightarrow \gamma$  transformation, which can be interpreted as cementite dissolution in austenite to reach equilibrium state. Such contraction was not observed for austenitization at lower temperatures. It is possible, that the cementite dissolution was finished during  $\alpha \rightarrow \gamma$  transformation for austenitization at temperatures 800 °C and lower. No significant cementite dissolution took place after  $\alpha \rightarrow \gamma$  transformation completion. Chromium diffusion controls austenitization rate at temperature 750 °C probably from the very beginning. That could be explanation for extreme drop in austenitization rate for 760 °C in comparison with austenitization at higher temperature (**Figure 7 G**).

#### 4. CONCLUSION

Austenitization behaviour of 100CrMnSi6-4 bearing steel was studied. Dilatometric analysis of isothermal austenitization proved, that two phenomena controls austenitization - carbon and chromium diffusion. Temperature 810 °C is sufficient for austenitization of whole volume of ferrite supported by cementite dissolution based only on carbon diffusion. Austenitization at lower temperatures requires besides carbon diffusion probably also chromium diffusion to obtain austenite/cementite structure. Chromium diffusion is significantly slower than carbon diffusion, thus the austenitization is retarded.

Cementite lamellae fragmented at advancing interphase boundary austenite/pearlite. The austenite grew into ferritic lamellae. Cementite lamellae dissolved partially and fragmented in narrow, 1µm across, zone at the interphase. The period of the fragmentation depends on velocity of austenite growth. It varied from 350 nm to 175nm for isothermal austenitization temperatures from 750 °C to 810 °C.

#### ACKNOWLEDGEMENTS

*This paper was created by project Development of West-Bohemian Centre of Materials and Metallurgy No.: LO1412, financed by the MEYS of the Czech Republic.*

**REFERENCES**

- [1] BHADESHIA, H.K.D.H. Steels for Bearings. *Progress in materials Science*, 2012, vol. 57, pp. 268-435.
- [2] HAUSEROVA, D., DLOUHY, J., NOVY, Z. Microstructure and Properties of Hardened 100CrMnSi6-4 Bearing Steel After Accelerated Carbide Spheroidization and Long-Duration Annealing. In *Bearing Steel Technologies: 10<sup>th</sup> Volume, Advances in Steel Technologies for Rolling Bearings*, 2015, pp. 389-409.
- [3] VERHOEVEN, J.D., GIBSON E.D. The Divorced Eutectoid Transformation in Steel, *Metallurgical and Material Transactions A*, 1997, vol. 29A, pp. 1181-1189.
- [4] SHTANSKY, D.V., NAKAI, K., OHMORI, Y. Pearlite to austenite Transformation in an Fe-2.6Cr-1C Alloy. *Acta Materialia*, 1999, vol. 47, no. 9, pp. 2619-2632.
- [5] ATKINSON, C., AKBAY, T., REED, R. C. Theory for reaustenitization from ferrite/cementite mixtures in Fe-C-X steels. *Acta Metallurgica et Materialia*, 1995, vol. 43, no. 5, pp. 2013-2031.